Effect of ro-vibrational excitation of NeH^+ on the stereodynamics for the reactions $H + NeH^+$ ($v = 1$–3, $j = 1,3,5$) $\rightarrow H_2^+ + Ne$*

Yin Shu-Hui(尹淑慧)[a)†], Zou Jing-Han(邹静涵)[a)], Guo Ming-Xing(郭明星)[b)], Li Lei(李 磊)[a)], Xu Xue-Song(许雪松)[a)], Gao Hong(高 宏)[a)], and Che Li(车 丽)[a)]

[a)] *Department of Physics, Dalian Maritime University, Dalian* 116026, *China*

[b)] *Environmental Science and Engineering College, Dalian Maritime University, Dalian* 116026, *China*

(Received 26 April 2012; revised manuscript received 19 July 2012)

The stereodynamics of the abstraction reaction $H + NeH^+$ ($v = 1$–3, $j = 1,3,5$) $\rightarrow H_2^+ + Ne$ is studied theoretically with a quasi-classical trajectory method on a new *ab initio* potential energy surface [Lü S J, Zhang P Y, Han K L and He G Z 2012 *J. Chem. Phys.* **132** 014303]. The effects of vibrational and rotational excitation of reagent molecules on the polarization of the product are investigated. The reaction cross sections, the distributions of $P(\theta_r)$, $P(\phi_r)$, and polarization-dependent differential cross sections (PDDCSs) are calculated. The obtained cross sections indicate that the title reaction is a typical barrierless atom (ion)–ion (molecule) reaction. The initial vibrational excitation and rotational excitation of reagent molecules have distinctly different influences on stereodynamics of the title reaction, and the possible reasons for the differences are presented.

Keywords: stereodynamics, quasi-classical trajectory, polarization, vibrational excitation, rotational excitation

PACS: 82.20.Bc, 82.20.Kh **DOI:** 10.1088/1674-1056/22/2/028201

1. Introduction

Vector property plays a vital part in understanding chemical reaction mechanisms. Vectors, such as velocities and angular momenta, possess not only magnitudes that can be directly related to translational and rotational energy, but also well-defined directions. Some pioneering investigations on dynamical stereo-chemistry can be found in Refs. [1]– [4]. Only by considering scalar and vector properties together can the fullest picture of the scattering dynamics emerge. The vector correlations between the reagent relative velocity vector $\boldsymbol{k}$ and product relative velocity vector $\boldsymbol{k}'$ are characterized by the differential cross section $(\mathrm{d}\sigma/\mathrm{d}\omega_t)$. Furthermore, the correlations of three vectors $\boldsymbol{k}$, $\boldsymbol{k}'$, and $\boldsymbol{j}'$ (the product rotational angular momentum) in the center of mass (CM) frame can be characterized by some double and triple vector correlations.[5] In the past two decades, Han and co-workers[6–11] measured the rotational alignments of products for a series of chemical reactions with the chemiluminescence and the laser-induced fluorescence techniques, and explored the product rotational polarizations of bimolecular reactions with different reagent mass combinations on attractive, mixed, and repulsive potential energy surfaces (PESs) by developing their own computational code. These authors, of whom some[6] were the first people to introduce the quasi-classical trajectory (QCT) method into the chemical stereodynamics field, also proposed the impulse model for explaining the polarization behaviors in a triatomic A + BC collision system.[11] Recently, the stereodynamical code developed by Han *et al.*[7–10] has been renewed and used successfully in many chemical reactions.[12–17] In the present work, we use this computational code to explore the product rotational polarization in the title reaction.

There have been very few investigations of the title reaction to date. However, its reverse reaction $Ne + H_2^+ \rightarrow NeH^+ + H$ has been studied in detail both experimentally and theoretically.[18–25] In 2010, Lü *et al.*[26] reported on a new *ab initio* potential energy surface (named LZHH PES hereafter) which accords fairly well with the experimental one. Based on LZHH PES, Xiao *et al.*[27] studied the product rotational angular momentum polarizations at different collision energies by using the QCT method. The isotopic effects on the stereodynamics of $Ne + H_2^+/Ne + HD^+/Ne + HT^+$ and $Ne + H_2^+/D_2^+/T_2^+$ were also studied with the QCT method[28,29] on the same LZHH PES. Wang *et al.*[30] carried out QCT calculations to investigate the stereodynamics of $Ne + H_2^+$ when reagent molecules are vibrationally excited, finding that the vibrational excitation of the reagent has a greater influence on the product rotational angular momentum polarization than the collision energy. Moreover, the study by Ge and Zheng[31] with the QCT method indicated that the NeH^+ product shows rotationally hot and vibrationally cold distributions. To shed more light on the title reaction, in this work we will adopt a QCT calculation on the new LZHH PES to investigate the product rotational angular momentum polarizations at different initial vibrational and rotational excitation levels. The remainder of this paper is organized as follows. In Section 2, the

*Project supported by the National Natural Science Foundation of China (Grant No. 11105022) and the Fundamental Research Funds for the Central Universities, China (Grant Nos. 2012QN066 and 2011QN142).

†Corresponding author. E-mail: yinsh@dlmu.edu.cn

© 2013 Chinese Physical Society and IOP Publishing Ltd

expressions for these stereodynamical quantities and relevant theory are given. In Section 3, results and discussion are presented. Finally, in Section 4 we draw some conclusions from this study.

2. Basic theory

2.1. Rotational polarization of the product

Figure 1 shows the CM frame, which is employed in the present calculation. The full three-dimensional (3D) angular distribution related $\boldsymbol{k}$–$\boldsymbol{k}'$–$\boldsymbol{j}'$ can be represented by a set of generalized polarization-dependent differential cross sections (PDDCSs) in the CM frame. The z axis of the CM frame is parallel to the reagent initial relative velocity vector $\boldsymbol{k}$ while the zx plane (the scattering plane) contains $\boldsymbol{k}$ and $\boldsymbol{k}'$ (the product final relative velocity vector). The angle θ_t is the so-called scattering angle between the reagent relative velocity and the product relative velocity. θ_r and ϕ_r are the polar and azimuthal angles of the final rotational angular momentum $\boldsymbol{j}'$. The fully correlated CM angular distribution is written in the form of the summation as[5]

$$P(\omega_t,\omega_r)=\sum_{kq}\frac{[k]}{4\pi}\frac{1}{\sigma}\frac{d\sigma_{kq}}{d\omega_t}C_{kq}(\theta_r,\phi_r)^*, \tag{1}$$

where $[k]\equiv(2k+1)$ $-k\le q\le k$, $(1/\sigma)(d\sigma_{kq}/d\omega_t)$ are the generalized PDDCSs,[8] $C_{kq}(\theta_r,\phi_r)$ are the modified spherical harmonics[32] and the differential cross section (DCS) is given by

$$\frac{1}{\sigma}\frac{d\sigma_{00}}{d\omega_t}\equiv P(\omega_t)=\sum_{k_1}\frac{[k_1]}{4\pi}h_0^{k_1}(k_1,0)P_{k_1}(\cos\theta_t). \tag{2}$$

The bipolar moment is evaluated using

$$h_0^{k_1}(k_1,0)=\langle P_{k_1}(\cos\theta_t)\rangle. \tag{3}$$

In the calculations, the truncated number in this expansion is $k_1=7$. The distribution function $P(\theta_r)$, the most common vector correlation, describing the $\boldsymbol{k}$–$\boldsymbol{j}'$ correlation, is expanded in a series of Legendre polynomials as[7]

$$P(\theta_r)=\frac{1}{2}\sum_k(2k+1)a_0^{(k)}P_k(\cos\theta_r), \tag{4}$$

where $[k]=(2k+1)$ and

$$a_0^{(k)}=\int_0^\pi P(\theta_r)P_k(\cos\theta_r)\sin\theta_r d\theta_r=\langle P_k(\cos\theta_r)\rangle, \tag{5}$$

with the expansion coefficients $a_0^{(k)}$ referred to as orientation (k is odd) or alignment (k is even) parameters, and $k=2$ indicates the product rotational alignment

$$a_0^2=\langle P_2(\cos\theta_r)\rangle=\langle P_2(\boldsymbol{j}'\cdot\boldsymbol{k})\rangle=\frac{1}{2}\langle 3\cos^2\theta_r-1\rangle. \tag{6}$$

In this study, we calculate only the average rotational alignment of the product, because it has been measured in most experiments. In the calculations, $P(\theta_r)$ is expanded up to $k=18$, which shows good convergence. The dihedral angle distribution function $P(\phi_r)$ describing the $\boldsymbol{k}$–$\boldsymbol{k}'$–$\boldsymbol{j}'$ correlation can be expanded in the Fourier series as

$$P(\phi_r)=\frac{1}{2\pi}\Big(1+\sum_{\text{even},n\ge2}a_n\cos(n\phi_r)+\sum_{\text{odd},n\ge1}b_n\sin(n\phi_r)\Big), \tag{7}$$

where

$$a_n=2\langle\cos(n\phi_r)\rangle, \tag{8}$$

$$b_n=2\langle\sin(n\phi_r)\rangle. \tag{9}$$

In this calculation, $P(\phi_r)$ is expanded up to $n=24$, which is sufficient for good convergence. Using angles θ_r and φ_r to determine the direction of $\boldsymbol{j}'$, the space distribution of the product rotation angular momentum can be written as

$$P(\theta_r,\phi_r)=\frac{1}{4\pi}\sum_{kq}[k]a_q^kC_{kq}(\theta_r,\phi_r)$$
$$=\frac{1}{4\pi}\sum_k\sum_{q\ge0}\left[a_{q\pm}^k\cos q\phi_r-a_{q\mp}^k\mathrm{i}\sin q\phi_r\right]C_{kq}(\theta_r,0). \tag{10}$$

The polarization parameter is evaluated as

$$a_{q\pm}^k=2\langle C_{k|q|}(\theta_r,0)\cos q\varphi_r\rangle, \tag{11}$$

$$a_{q\mp}^k=2\mathrm{i}\langle C_{k|q|}(\theta_r,0)\cos q\varphi_r\rangle. \tag{12}$$

In the calculations, $P(\theta_r,\ \phi_r)$ is expanded to $k=7$, which is sufficient for good convergence.

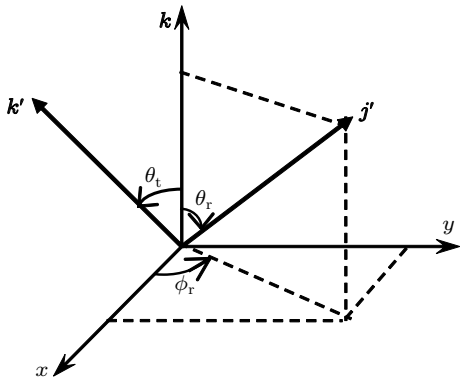


Fig. 1. Center-of-mass frame used to describe the $\boldsymbol{k}$, $\boldsymbol{k}'$, $\boldsymbol{j}'$ correlations.

2.2. Potential energy surface

In the present calculations, we use a new 3D adiabatic PES for the ground state ($1^2A'$) of HNeH system constructed by Lü *et al.*[26] The PES is computed using the complete active space self-consistent field (CASSCF) and internally contracted multireference configuration interaction (MRCI) wave function with aug-cc-pv5z basis set of Dunning.[33] The analytical representation of the PES is fitted with 7026 *ab initio* energies below 2.8 eV relative to the dissociation energy of $Ne+H_2^+$ and represented by the Aguado–Paniagua function.[34] The LZHH PES features a deep well in the collinear configuration, and no other wells or barriers are found for this configuration. The depth of well becomes shallower and a barrier appears when the Ne–H–H angle is reduced.

2.3. QCT calculations

The classical Hamilton equations are numerically integrated in three dimensions, of which the accuracy is verified by checking the conservations of total energy and total angular momentum for each trajectory. The drawback of the QCT method is that it is incapable of treating quantum-mechanical effects, such as the zero-point energy problem, tunneling, resonance, and non-adiabatic transitions. To consider the zero-point energy, a passive method of discarding all reactive trajectories which form products with a total vibrational energy lower than the total harmonic zero-point energy of the products is used. The collision energy (E_c) is chosen to be 0.5 kcal/mol in this work. To investigate the effect of vibrational excitation on the product polarization, the initial vibrational level and rotational level are taken to be $v = 1,2,3$ and $j = 0$, respectively. To explore the effect of rotational excitation, we choose the vibrational level and rotational levels to be $v = 0$ and $j = 1,3,5$, respectively. In this calculation, batches of 10^5 trajectories are run for each reaction and integration step size is chosen to be 0.1 fs. The trajectories each are started at an initial distance of 10 Å (1 Å = 0.1 nm) between the H atom and the center of the mass of the NeH^+ molecule.

3. Results and discussion

Figure 2 presents the total cross section summed over the final rovibrational states of products as a function of collision energy ranging from 0.5 kcal/mol to 30 kcal/mol. From Fig. 2, it can be seen that the value of the cross section decreases with the increase of collision energy. The cross section curve shows the characteristics of a typical barrierless atom (ion)–ion (molecule) reaction. Namely the maximum value is at $E_c = 0$ kcal/mol and decreases with the increase of collision energy, which accords well with the exothermic property of the title reaction.

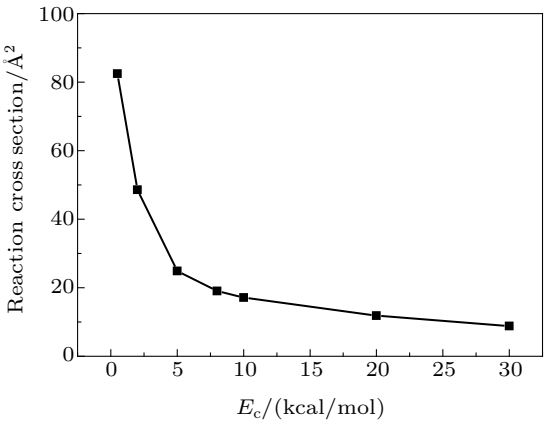


Fig. 2. QCT-computed reaction cross sections each as a function of collision energy ranging from 0.5 kcal/mol–30 kcal/mol for the reaction $H + NeH^+$ ($v = 0$, $j = 0$) $\rightarrow H_2^+ + Ne$.

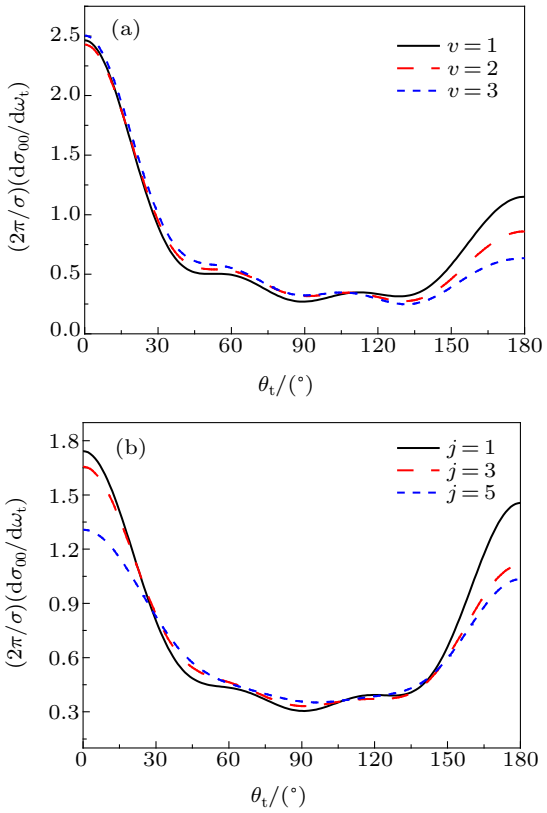


Fig. 3. (color online) Differential cross sections for $H + NeH^+$ ($v = 1$–3, $j = 1,3,5$) $\rightarrow H_2^+ + Ne$ at $E_c = 0.5$ kcal/mol, of which each is plotted as a function of scattering angle.

The PDDCS $(2\pi/\sigma)(d\sigma_{00}/d\omega_t)$ is simply the differential cross section (DCS), which describes the $\boldsymbol{k}$–$\boldsymbol{k}'$ correction. It just reflects the scattering direction and is not associated with the orientation and alignment of final rotational angular momentum $\boldsymbol{j}'$. The DCSs for the three initial vibrational states $v = 1,2,3$ when $j = 0$ and for the three initial rotational states $j = 1,3,5$ when $v = 0$ are presented in Figs. 3(a) and 3(b), respectively. The collision energies in the two figures are selected to be 0.5 kcal/mol. From Fig. 3, the significant differences can be seen and will be discussed below. The curves in Fig. 3(a) are asymmetric, which show that the products present mainly forward and backward scattering, and the forward scattering is stronger than the backward one. Moreover, the vibrational excitations of reagents will weaken backward scattering and augment the asymmetry. In contrast, the curves in Fig. 3(b) are more symmetric. The forward scattering is slightly stronger than the backward one, and the values at $\theta_t = 0^\circ$ and $\theta_t = 180^\circ$ decline when reagent molecules are at higher rotational states. The sharp difference between Fig. 3(a) and Fig. 3(b) is very interesting. The possible reason is that the vibrational excitations of reagent molecules increase the internal energy of system, causing the product molecules to move with less effect of the well. From previous studies, it can be seen that the existing well on the PES leads to the forward and backward scatterings. So, it is no surprise that the angular distribution becomes less isotropic when reagent molecules are in the vibrational excitation. However, when

reagent molecules are in the rotational excitation, the trajectories may deviate from the optimal reaction path. As a result, the system spends more time in the interaction region and both forward scattering and backward scattering decrease.

Figure 4(a) shows $P(\theta_r)$ distributions at $E_c = 0.5$ kcal/mol for the three initial vibrational states $v = 1, 2$, and 3 with the ground initial rotational state $j = 0$. From Fig. 4(a), the $P(\theta_r)$ distributions peak at θ_r angles close to 90° and are symmetric with respect to 90°, which demonstrates that the product rotational angular momentum $\boldsymbol{j}'$ is distributed with cylindrical symmetry in the product scattering frame, and the direction of $\boldsymbol{j}'$ has a preferential alignment perpendicular to $\boldsymbol{k}$ direction. With the increase of the vibrational excitation level, these distributions show some differences in shape. The peaks at $\theta_r = 90°$ have slight increases with the reagent molecules NeH^+ being excited to higher vibrational states. Figure 4(b) reveals the $P(\theta_r)$ distributions for different initial rotational levels. From Fig. 4(b), it can be seen that the $P(\theta_r)$ distributions also peak at $\theta_r = 90°$, while the values of the peak decrease with initial molecules being excited to higher rotational states. The $P(\theta_r)$ distributions also show oscillation behaviors which become apparent when reagent molecules are at higher rotational excitation levels. The decrease of the peak in $P(\theta_r)$ distribution may be due to the rotation of reagent molecules, which results in the deviations of some trajectories from the optimal reaction path thus weakening the alignment of $\boldsymbol{j}'$.

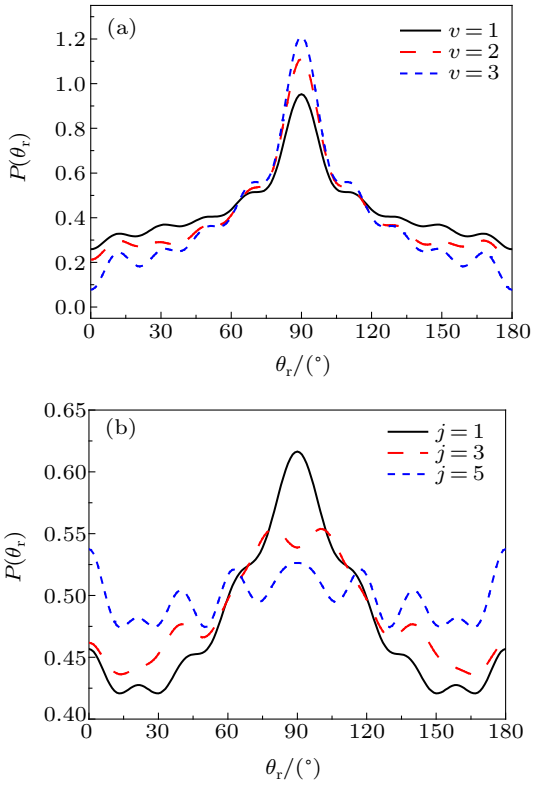


Fig. 4. (color online) Angular distributions of $P(\theta_r)$ reflecting the $\boldsymbol{k}$–$\boldsymbol{j}'$ correlation for the title reaction. (a) NeH^+ is at $v = 1, 2, 3$, $j = 0$. (b) NeH^+ is at $j = 1, 3, 5$, $j = 0$.

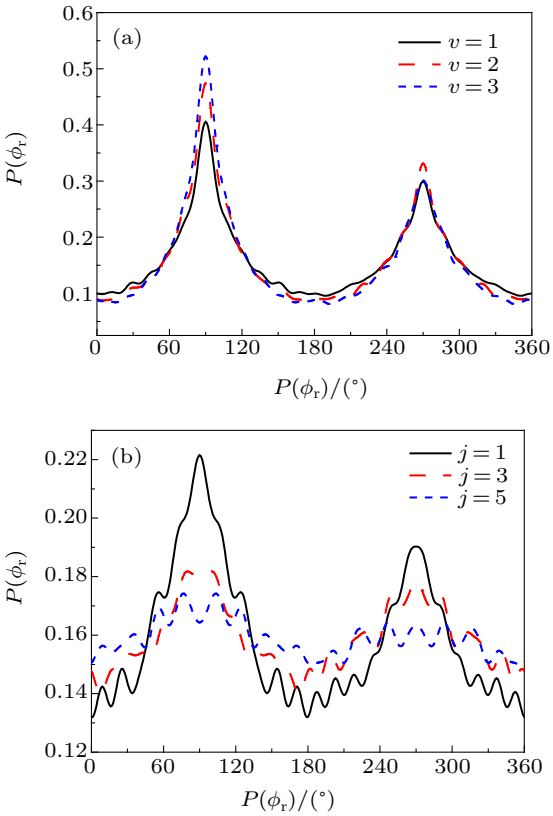


Fig. 5. (color online) Angular distributions of $P(\phi_r)$ reflecting the $\boldsymbol{k}$–$\boldsymbol{k}'$–$\boldsymbol{j}'$ correlation for the title reaction. (a) NeH^+ is at $v = 1, 2, 3$, $j = 0$. (b) NeH^+ is at $j = 1, 3, 5$, $j = 0$.

Figure 5 illustrates the influence of rovibrational excitation on the orientation of product rotational angular momentum $\boldsymbol{j}'$. The dihedral angle distribution $P(\phi_r)$ describes the $\boldsymbol{k}$–$\boldsymbol{k}'$–$\boldsymbol{j}'$ correlations. Some similar characteristics can be found from Fig. 5 below.

(i) the $P(\phi_r)$ distributions are asymmetric with respect to the $\boldsymbol{k}$–$\boldsymbol{k}'$ scattering plane, directly reflecting the strong polarization of $\boldsymbol{j}'$;

(ii) the peaks of $P(\phi_r)$ appear at $\phi_r = 90°$ and 270°, which shows that the $\boldsymbol{j}'$ of product H_2^+ is aligned mainly along the y axis of the CM frame;

(iii) the peaks at $\phi_r = 90°$ are stronger than those at $\phi_r = 270°$, indicating that $\boldsymbol{j}'$ is not only aligned, but also oriented along the positive direction of y axis.

It is noteworthy that the distributions of $P(\theta_r)$ are symmetric, while the distributions of $P(\phi_r)$ are asymmetric. The "impulsive-collision model" of atom and molecule reaction A+BC→AB+C, developed by Han *et al.*[11,35] can well account for this asymmetry. The product rotational angular momentum $\boldsymbol{j}'$ can be expressed as $\boldsymbol{j}' = \boldsymbol{L}\sin^2\beta + \boldsymbol{j}\cos^2\beta + \boldsymbol{J}_1 m_B/m_{AB}$, where $\boldsymbol{L}$ and $\boldsymbol{j}$ are the orbital and rotational angular momentums of the reactant molecule BC, respectively. $\boldsymbol{J}_1 = \sqrt{\mu_{BC}R}(\boldsymbol{r}_{AB} \times \boldsymbol{r}_{CB})$, where $\boldsymbol{r}_{AB}$ and $\boldsymbol{r}_{CB}$ are unit vectors in the B–A and B–C directions, respectively. The μ_{BC} is the reduced mass of the BC molecule and R is the repulsive energy between B and C atoms. During the chemical bond forming and breaking for the title reaction, the term

$\boldsymbol{L}\sin^2\beta + \boldsymbol{j}\cos^2\beta$ in the equation is symmetric with respect to the $\boldsymbol{k}$–$\boldsymbol{k}'$ scattering plane, whereas the term $\boldsymbol{J}_1 m_{\rm B}/m_{\rm AB}$ has a preferred direction because of the effect of the repulsive energy R, which causes the orientation of the products H_2^+. However, the vibrational excitations and rotational excitations of reagent molecules have distinctly different effects on product orientation. Figure 5(a) shows the $P(\phi_{\rm r})$ distributions at $E_{\rm c} = 0.5$ kcal/mol when reagents are excited to higher vibrational states. The peaks at $\phi_{\rm r} = 270°$ almost remain unchanged, while the peaks at $\phi_{\rm r} = 90°$ rise with higher initial vibrational states. The results denote the product orientation is enhanced by vibrational excitations of reagent molecules. In comparison, figure 5(b) shows that the peaks at $\phi_{\rm r} = 90°$ and $\phi_{\rm r} = 270°$ both become lower and broader when the rotational excitations of reagent molecules are enhanced. We will use the term "in-plane" to refer to the preference of the product molecule rotating in the plane parallel to the scattering plane, whereas the term "out-of-plane" is to refer to the preference of the product molecule rotating in the plane perpendicular to the scattering plane. The peaks at higher rotational levels are broader, which demonstrates the rotation of product molecules has a preference of changing from the "in-plane" reaction mechanism to the "out-of-plane" mechanism. However the same behavior is not obvious when reagent molecules are excited to higher vibrational levels.

Figures 6 and 7 show the other three polarization-dependent differential cross sections ($(2\pi/\sigma)(\mathrm{d}\sigma_{20}/\mathrm{d}\omega_{\rm t})$, $(2\pi/\sigma)(\mathrm{d}\sigma_{22+}/\mathrm{d}\omega_{\rm t})$, and $(2\pi/\sigma)(\mathrm{d}\sigma_{21-}/\mathrm{d}\omega_{\rm t})$) when the reagent molecules are in the vibrational and rotational excitation, respectively. The polarization-dependent differential cross sections $(2\pi/\sigma)(\mathrm{d}\sigma_{20}/\mathrm{d}\omega_{\rm t})$ is related to the expectation value of the second Legendre moment $\langle P_2(\cos\theta_{\rm r})\rangle$, which can be obtained by $(2\pi/\sigma)(\mathrm{d}\sigma_{20}/\mathrm{d}\omega_{\rm t})$ normalized with the differential cross section $(2\pi/\sigma)(\mathrm{d}\sigma_{00}/\mathrm{d}\omega_{\rm t})$, and the polarization-dependent differential cross sections $(2\pi/\sigma)(\mathrm{d}\sigma_{22+}/\mathrm{d}\omega_{\rm t})$ and $(2\pi/\sigma)(\mathrm{d}\sigma_{21-}/\mathrm{d}\omega_{\rm t})$ are related to $\langle\sin^2\theta_{\rm r}\cos 2\varphi_{\rm r}\rangle$ and $\langle-\sin 2\theta_{\rm r}\cos\phi_{\rm r}\rangle$, respectively. The effect of vibrational excitation on PDDCSs can be examined by comparing the results in Figs. 6(a)–6(c). The behavior of $(2\pi/\sigma)(\mathrm{d}\sigma_{20}/\mathrm{d}\omega_{\rm t})$, which is shown in Fig. 6(a), has the opposite trend to that of $(2\pi/\sigma)(\mathrm{d}\sigma_{00}/\mathrm{d}\omega_{\rm t})$ in Fig. 3(a), reflecting that $\boldsymbol{j}'$ is strongly aligned along the direction perpendicular to $\boldsymbol{k}$. The alignment of products strengthens with the increase of the initial vibrational states. Moreover, $\boldsymbol{j}'$ is preferentially polarized along the direction perpendicular to $\boldsymbol{k}$ at $\theta_{\rm t} = 0°$ and $\theta_{\rm t} = 180°$. It is obvious that the PDDCSs with $q \neq 0$ are equal to zero at the extremities of forward and backward scattering. At these limited scattering angles, the $\boldsymbol{k}$–$\boldsymbol{k}'$ scattering plane is not determined and the values of these PDDCSs with $q \neq 0$ must be zero.[36] As shown in Fig. 6(b), the values of $(2\pi/\sigma)(\mathrm{d}\sigma_{22+}/\mathrm{d}\omega_{\rm t})$ in the whole scattering angle range (except for extremities of forward and backward scattering) are negative, implying that there is a preference for $\boldsymbol{j}'$ to be aligned along the y axis. The strongest polarizations of the product molecules are all at about $\theta_{\rm t} = 30°$, and the absolute values increase when the reagents are excited to higher vibrational levels. The effect of vibrational excitation on $(2\pi/\sigma)(\mathrm{d}\sigma_{21-}/\mathrm{d}\omega_{\rm t})$ distribution is plotted in Fig. 6(c). The values of $(2\pi/\sigma)(\mathrm{d}\sigma_{21-}/\mathrm{d}\omega_{\rm t})$ are negative in the forward hemisphere, and positive in the backward hemisphere. This behavior indicates that $\boldsymbol{j}'$ is along the direction of $x+z$ at forward scattering angles and along the direction of $x-z$ at the backward scattering angles.

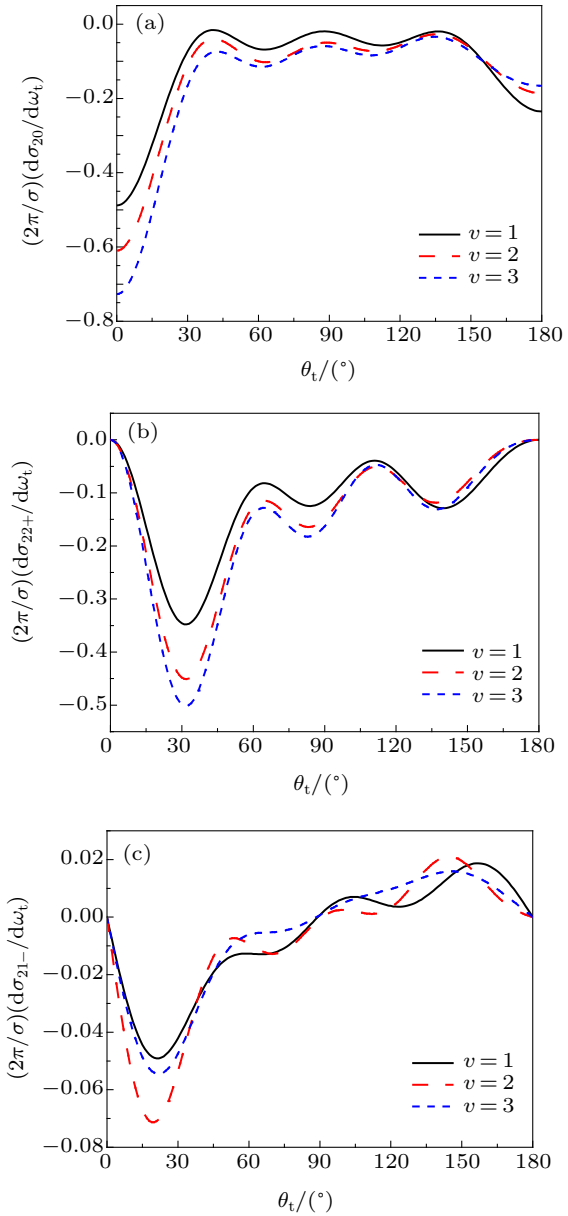


Fig. 6. (color online) PDDCSs with $(k,q) = (2,0),(2,2+),(2,1-)$ for the reaction $H + NeH^+$ ($v = 1$–3, $j = 0$) $\rightarrow H_2^+ + Ne$ at $E_{\rm c} =$ 0.5 kcal/mol.

Figure 7 shows the rotational excitations of reagent molecules. The distribution of $(2\pi/\sigma)(\mathrm{d}\sigma_{20}/\mathrm{d}\omega_{\rm t})$ demonstrates that $\boldsymbol{j}'$ has a strong alignment along the direction perpendicular to $\boldsymbol{k}$, whereas the degree of alignment decreases with the number of initial rotational states increasing. The behavior of $(2\pi/\sigma)(\mathrm{d}\sigma_{20}/\mathrm{d}\omega_{\rm t})$ distribution is con-

sistent with that of $P(\theta_r)$ distribution in Fig. 4(b). The $(2\pi/\sigma)(d\sigma_{22+}/d\omega_t)$ distribution and $(2\pi/\sigma)(d\sigma_{21-}/d\omega_t)$ distribution display more isotropic behaviors when reagent molecules are excited to higher rotational levels. Furthermore, the polarizations of products in the title reagent are more sensitive to initial rotational excitation rather than vibrational excitation. We are eagerly looking forward to the experimental studies of the stereodynamics for the title reaction, so that a comparison can be made between theory and experiment.

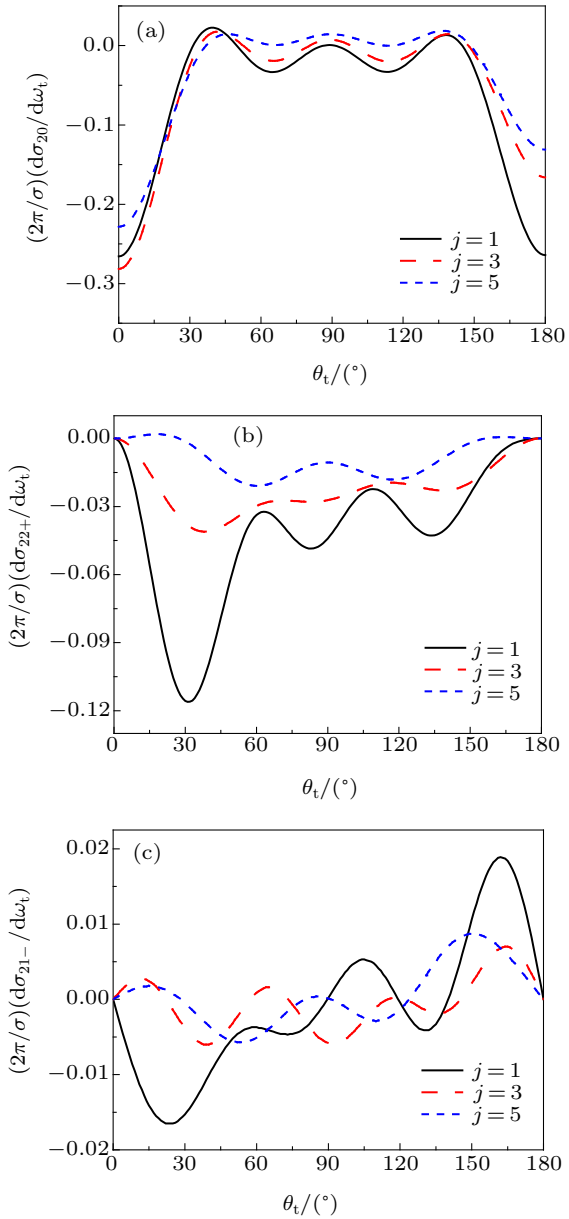


Fig. 7. (color online) PDDCSs with $(k,q)=(2,0),(2,2+),(2,1-)$ for the reaction $H+NeH^+$ $(j=1,3,5, v=0) \rightarrow H_2^+ + Ne$ at $E_c = 0.5$ kcal/mol.

4. Conclusions

To explore the product rotational angular momentum polarization in the $H+NeH^+$ $(v=1$–$3,\ j=1,3,5) \rightarrow H_2^+ + Ne$ reaction, the angular distributions $P(\theta_r)$, $P(\phi_r)$, and four PDDCSs are obtained by quasi-classical trajectory calculations. The vibrational and rotational excitations of reagent molecules have remarkably different influences on the title reaction. When the reagents are at vibrational excitation levels, the products preferentially present forward scattering, and the degree of backward scattering becomes weaker with the number of initial vibrational levels increasing. The product rotational angular momentum $\boldsymbol{j}'$ is not only aligned along the direction perpendicular to the scattering plane but also oriented along the positive direction of the y axis. The degrees of alignment and orientation of $\boldsymbol{j}'$ are enhanced by the initial vibrational excitation. In the condition of initial rotational excitation, the products present mainly forward and backward scattering, and the degree of the forward scattering is stronger than that of the backward one. The rotational excitations of reagent molecules will lead to the decline in both forward and backward scattering. The alignment and orientation of $\boldsymbol{j}'$ fade out, owing to the rotational excitations of initial molecules. The PDDCSs are investigated when reagent molecules are in vibrational excitation and rotational excitation, which show that the polarization of the product is more sensitive to rotational excitation. The calculated cross sections indicate that the title reagent is a typical barrierless atom (ion)–ion (molecule) reaction .

Acknowledgement

The authors are grateful to professor Han K L for providing the potential energy surface.

References

[1] Fano U and Macek J H 1973 *Rev. Mod. Phys.* **45** 553
[2] Case D A and Herschbach D R 1975 *Mol. Phys.* **30** 1537
[3] Mcclelland G M and Herschbach D R 1979 *J. Phys. Chem.* **83** 1445
[4] Barnwell J D, Loeser J G and Herschbach D R 1983 *J. Phys. Chem.* **87** 2781
[5] Aoiz F J, Brouard M and Enriquez P A 1996 *J. Chem. Phys.* **105** 4964
[6] Han K L, He G Z and Lou N Q 1993 *Chin. Chem. Lett.* **4** 517
[7] Han K L, He G Z and Lou N Q 1996 *J. Chem. Phys.* **105** 8699
[8] Wang M L, Han K L and He G Z 1998 *J. Chem. Phys.* **109** 5446
[9] Wang M L, Han K L and He G Z 1998 *J. Phys. Chem.* A **102** 10204
[10] Zhang X and Han K L 2006 *Int. J. Quantum Chem.* **106** 1815
[11] Li R J, Han K L, Li F E, Lu R C, He G Z and Lou N Q 1994 *Chem. Phys. Lett.* **220** 281
[12] Yin S H, Guo M X, Li L, Zhang Y H and Li X P 2011 *Int. J. Quantum Chem.* **111** 4400
[13] Li H, Zheng B, Yin J Q and Meng Q T 2011 *Chin. Phys.* B **20** 123401
[14] Liu Y F, He X H, Shi D H and Sun J F 2011 *Chin. Phys.* B **20** 078201
[15] Chen Y Y and Zhao M Y 2012 *J. Theor. Comput. Chem.* **11** 87
[16] Chen X Q, Wang M S, Yang C L and Wu J C 2012 *Chin. Phys.* B **21** 023402
[17] Xie T X, Li S J, Shi Y and Jin M X 2012 *Chin. Phys.* B **21** 013401
[18] Bilotta R M and Farrar J M 1981 *J. Chem. Phys.* **75** 1776
[19] Van Pijkeren D, Boltjes E, van Eck J and Niehaus A 1984 *Chem. Phys.* **91** 293
[20] Herman Z and Koyano I 1987 *J. Chem. Soc., Faraday Trans.* **83** 127
[21] Zhang T, Qian X M, Tang X N, Ng C Y, Chiu Y, Levandier D J, Miller J S and Dressler R A 2003 *J. Chem. Phys.* **119** 10175
[22] Kress J D, Walker R B, Hayes E F and Pendergast P 1994 *J. Chem. Phys.* **100** 2728
[23] Gilibert M, Blasco R M, González M, Giménez X, Aguilar A, Last I and Baer M 1997 *J. Phys. Chem.* A **101** 6821
[24] Gilibert M, Giménez X, Huarte-Larrañaga F, González M, Aguilar A, Last I and Baer M 1999 *J. Chem. Phys.* **110** 6278
[25] Mayneris-Perxachs J and González M 2009 *J. Phys. Chem.* A **113** 4105

[26] Lü S J, Zhang P Y, Han K L and He G Z 2010 *J. Chem. Phys.* **132** 014303
[27] Xiao J, Yang C L, Wang M S and Ma X G 2011 *Chin. Phys. Lett.* **28** 013101
[28] Xiao J, Yang C L, Wang M S and Ma X G 2011 *Chem. Phys.* **379** 46
[29] Xiao J, Lu Y C and Wang M S 2012 *Chin. Phys.* B **21** 043101
[30] Wang Y L, Tian B G, Qu L S, Chen J N and Li H 2011 *Bull. Korean Chem. Soc.* **32** 12
[31] Ge M H and Zheng Y J 2011 *Chin. Phys.* B **20** 083401
[32] Brouard M, Lambert H M, Rayner S P and Simons J P 1996 *Mol. Phys.* **89** 403
[33] Kendall R A, Dunning T H and Harrison R J 1992 *J. Chem. Phys. Lett.* **96** 6796
[34] Aguado A and Paniagua M 1992 *J. Chem. Phys.* **96** 1265
[35] Han K L, Zhang L, Xu D L, He G Z and Lou N Q 2001 *J. Phys. Chem.* A **105** 2956
[36] Gómez-Carrasco S, Hernándezb M L and Alvari J M 2007 *Chem. Phys. Lett.* **435** 188